Impact of GFRP Reinforcement Ratios on the Behavior of Full-Scale Concrete Bridge Deck Slabs

The NLFEA (non-linear finite element analysis) procedure consisted of preparing (12) bridge's slab models in order to evaluate the impact of the study's parameters, namely: 1) the ratio of transversal reinforcement at the bottom (ρ), and 2) the concrete's strength. To make the process easier, the ratio of the at-the-bottom reinforcement was set at: 0.38, 0.46, and 0.57; while the values of the strength of concrete were set at: 20, 30, 40, and 50 MPa. The findings showed that the majority of the experimented models experienced a punching shear mode of failure, along with a closely identical patterns of cracking. The research found that the at-tension strains were mostly governed by the ratio of the at-bottom transversal reinforcement. Also, it was found that strengthening the slab models with bars of glass-FRP impacted positively the at-ultimate load, elastic stiffness, stiffness after cracking, elastic energy absorption, and after-cracking energy; whereas, the reinforcement's influence on the at-ultimate deflection was merely noticeable in comparison with the models strengthened with steel bars. Further, the research found that the glass-FRP bars became more efficient when the level of the damage-by-heat was raised.

Keywords: *Reinforcement Ratio; GFRP bars; Bridge deck slabs; NLFEA; Strain*

Introduction

Lately, the bars of FRP (i.e., fiber-reinforced polymer) have been utilized, overwhelmingly, to strengthen elements of concrete in many applications, for example: highways, bridges, etc. **[1, 2]**. Nevertheless, these bars have a number of setbacks, as they are: considerably costly, poor in ductility, poor in mechanical qualities regarding resin, un-predictable in failure (brittle mode of failure), low in shear strength, and highly impacted by excessive temperatures (concerning strength as well as stiffness); such setbacks must be accounted for when erecting bars of FRP **[3, 4]**. In addition, the detrimental impact of excessively-high temperatures, resulted from arbitrary fire attacks, on FRP must be taken into serious consideration upon designing so as to widen and popularize the use of this material **[5, 6]**. In fact, little data is available with regard to the strengthened-with-FRP constructions' resistance to fire attacks, which is represented by: the structure's ability to withstand fire attacks without harming its integrity; also, no much data is available related to the bad effect of high temperature on the bonding's quantity, and structural strength as well as stiffness **[7, 8]**.

Compared with concrete elements, the in-bridge deck slabs are more often subjected to bad influences of environment, de-icing, adding to heavy load of traffic. These factors cause a quicker degradation to the bridge systems, which makes these systems to be continuously rehabilitated to avoid disastrous failure. In general, there are many structures located in "un-friendly" locations which makes

them vulnerable to risks, for example: bridges' decks and parking lots are often subjected to materials used for de-icing; the located-in-marine-surrounding structures and tunnels are often subjected to seawater; while the facilities in industrial areas are always subjected to chemical substances. Such structures are often reinforced with bars of glass-FRP. By time, the bars of glass-FRP have successfully been used instead of the steel bars, because the former are: anti-corrosion, light-weighted, cost-effective, stronger in tension, and easier to install in all kinds of structures, even in ones with complex geometry or those which contain magnetic resonance equipment and alike equipment. Additionally, regarding the life of service, the strengthened-with- glassFRP buildings do not need much maintenance or repair which saves much money **[9, 10]**. Despite the aforementioned advantages, there are still some worries regarding the response of reinforced-with-FRP RC structures to elevated levels of temperature. Actually, the FRP rebar's mechanical qualities as well as bond's properties are detrimentally impacted by extremely high temperatures. The American Society of Civil Engineers (ASCE) stated that their statistics had shown that the following five years would witness an increase in issues regarding civil infrastructures, costing more than a trillion and a half American Dollars. Canada, in particular, had in 2004 many deficient infrastructures that needed nearly sixty billion American Dollars. Researches **[11-17]** have been conducted to examine the behavior of RC with-continuous-slab bridges by creating a structural deterioration reliability model; they revealed that when the concrete cover was decreased, the potential of failure enhanced. Also, the interrelation and interaction among the diffused chlorides, transversely-appearing cracking, as well as the emergence of corrosion all were indicators that the structural reliability and the serviceability one both significantly reduced when the salts of de-icing were applied. A model of reliability was constructed for a concrete bridge's deck slab, including the changes (spatially and temporally) in the rate of corrosion. The construction of the model was done utilizing the Monte Carlo method of simulation and the computerized reliability model; then, the model was put to a comparison with a sophisticated model of reliability, along with a number of sub-models to explore the variation in the influence of load on the bridge slab's resistance through time. This model gave more accurate prediction for the bridge slab model's life of service **[11-17].**

Upon enhancing the structure's complexity of response, the experimental work will be more: expensive, time consumer, and require more labor **[18-22]**. A considerable number of researchers adopted the NLFEA method to evaluate and analyze the response of real-size RC bridge's deck slabs. Thus, the research in hand has followed the same path, as it presented a sophisticated simulated-through-NLFEA, damaged-by-excessive-heat bridge slab's model to predict: the patterns of cracking, structure's response, and failure's mode, noting that the model was reinforced, from internal side, with bars of FRP. The FE joint model was first put to validation with respect to first to the findings achieved by Bouguerra et al. **[23]**. After that, the model was enlarged to examine the influence of the research's parameters, which were: the ratio of at-bottom transversal reinforcement (ρ) and the concrete's strength.

Non-linear Finite Element Analysis (NLFEA)

Experimental Work Review

The experiment of Bouguerra et al. **[23]** has been employed in order to calibrate and validate the FE model of the research in hand. Eight models of actual-size concrete bridge's deck slabs were prepared, having a length of 3000 mm, a width of 2500 mm, and a thickness of (150, 175, and 200-mm). The support of the models consisted of a couple of parallel girders of steel, with a c-to-c spacing of 2000 mm (**Figure 1(a)**).

Description of NLFEA

Type of Elements

The 3-D element of Solid65 was employed for the sake of modeling the concrete's nonlinear-in-nature response; the reason of employing this element was that it was able to predict the each of in-tension cracking, in-compression crushing, in addition to plastic deformation **[24]**. Actually, this element had the viability of modeling strengthened/un-strengthened solid objects; also, the element of Solid65 had (8) defining nodes, as every node had 3 DoFs (degrees of freedom).

Figure1. *Typical dimensions of the tested slabs*

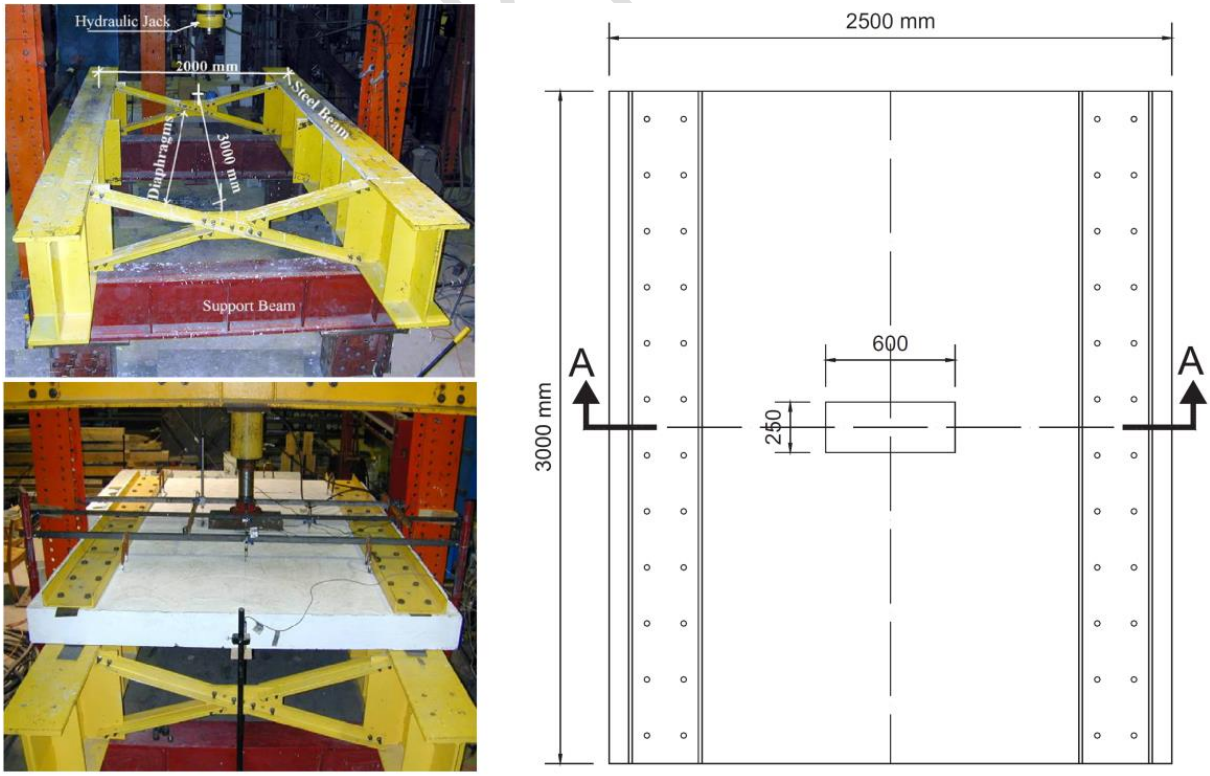

(a) The dimensions of the experimented slab models **[23]**

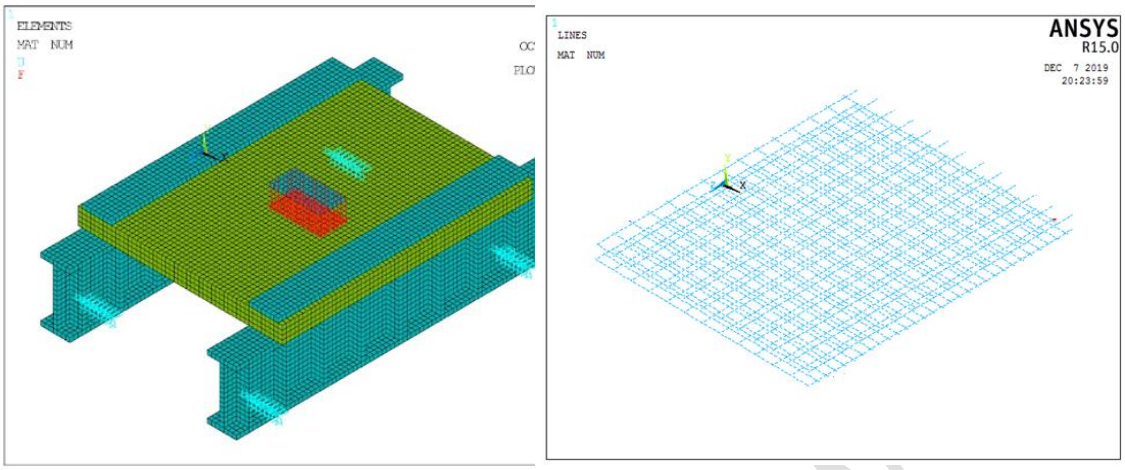

(b) NLFEA **[18]**

The element of LINK80 was used to model the each of: the reinforcing bars of FRP, reinforcing steel, bolts, and X bracing; this linking element had two 3-DoF nodes at the edges. Link180 was a three-dimensional uniaxial tension-compression spar, and had the ability to predict the each of: plasticity, rotations, large-sized strains, as well as deflections.

Further, the element of SOLID185 was employed to model the steel parts, i.e.: girders, channels, and plates of loading. This element had (8) defining with-3-DoF nodes. The material of the steel parts was simulated as homogenous solid.

Materials' Properties

Concrete: it was simulated utilizing the element of SOLID65, a solid type that had eight with-three-DoF nodes; the nodes could move in all orientations. The element had the capability of predicting, in three perpendicular orientations, the each of: cracks, crushing, and plastic deformations. It is worth mentioning the Solid65 element's ability to predict the concrete's crushing failure had been left out because it was not noticed during the experimental work. The concrete had: in-compression strength of: 30, 40, and 50 MPa; a Poisson's ratio of 0.2 (since the typical ratio was between 0.15 and 0.22) **[25]**. The coefficient of shear transfer (βt) was 0.2, as this coefficient defined the condition of the side of cracking, and the chosen value was universal **[25-27]**. To make sure that the FE model was accurate, Kent and Park **[28]** presented a formula to determine the concrete's compressive stress-strain relation.

FRP material: the bars of glass-FRP were simulated utilizing the element of Link180, where every one of this element's nodes had the capability of plastically deforming and translating in every orientation. The material of the glass-FRP consisted of two constituents highly-strong fibers implanted in a polymer matrix to make the fibers homogeneous and their response anisotropic. The glass-FRP's mechanical qualities were as following: the modulus of elasticity was 41.6 GPa, the at-ultimate strength in tension was 796 MPa, the Poison's ratio was 0.33**[23]**, and the at-ultimate strain in tension was 1870×10^{-6}.

Criteria of Failure and Procedure of Analysis

As stipulated, a structural element encounters a failure if the prime stress, in compressive or in tension, emerges out of the failure's side, regardless the direction of the stress **[29]**. The each of the concrete bridge slabs' ends had a condition of fixed-fixed. The applying of load was on steel plates, located at the slab's center, as the line of loading was all over sixty nodes. The plates of steel were utilized to prevent the stress from being concentrated at the slab's mid point and, also, to make a simulation for the load of truck exerted on the slab. The model was constrained by availing conditions of displacement boundary conditions. The displacement factors of Ux, Uy, and Uz were all zeroed at the girders' ends to make sure that the supports were fastened fixed at the two sides so as to imitate the experimentally-set boundary's conditions. In the beginning, the NLFEA needed to mesh the simulated model. To state it differently, the FE model was dividend to a number of smaller-in-size elements (25 mm); after the load was applied, the values of strains and stresses were computed at the elements' points of integration **[30]**. **Figure 1(b)** displays the typically-constructed mesh required for the FE models. Perfect bonding was presumed for the bonds of: concrete-steel, concrete-FRP, concrete slab-steel beam, as well as steel plates. The load was added, in an incremental manner, to prevent the solution from diverging; in result, extra increments of load were added at the phases of: appearance of initial crack, yielding of steel, and after-crushing. A convergence of solution, at the load-steps' ends, was achieved by utilizing the Newton-Raphson equilibrium iterations at the end of every increment of load, with a limit of tolerance of 0.001 at 0.35 kN. The sizes of the load increments were obtained, automatically, by ANSYS **[24]** for highest and lowest size of load increments. The simulated models failed when the at-0.0035kN-load-increment solution did not converge.

Validation

The FE results and the experimentally-obtained ones **[23]** were put in a comparison with each other, with regard to the graphs of load vs deflection (**Figure 2**). **Figure 2** indicated that the FE graphs of load vs deflection excellently agreed with the experimentally-obtained ones **[23]**. Further, the same figure indicated that the simulated-through-NLFEA RC slab models were nearly identical to the experimented ones with <10% error, except for the G-175-N-0.35 model which had < 20 error. Thus, in the light that the outcomes of the the simulated-via-FEA models were real close to the experimentally-achieved ones **[23]**, the simulated models were extended so as to explore the influence of various parameters utilizing NLFEA.

Figure 2. *Typical graphs of load vs mid-span deflection, experimental* ***[23]*** *and NLFEA's*

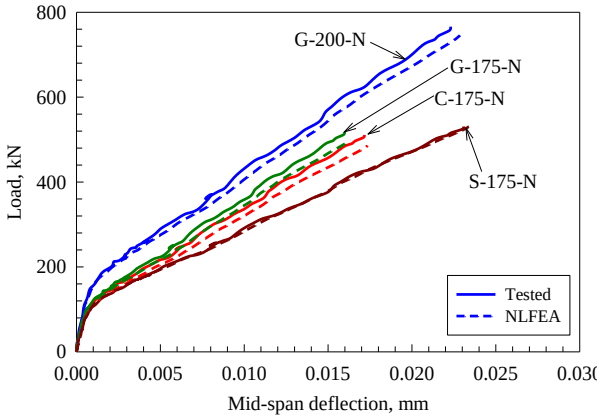

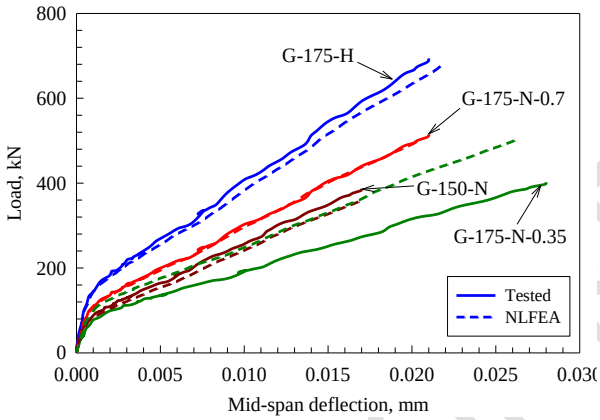

Research Parameters

A total of (12) simulated-through-NLFEA models were devised in order to investigate the impact of a number of parameters under concentrated loading, as demonstrated in **Table 1**.

Table 1. *Research parameters and NLFEA's outcomes*

Specimen	Concrete strength, MPa	Reinforcement ratio ,%	Δu, m	Pu, kN	Δcr, m	Pcr, kN
C50ρ0.57	50	0.57	0.01856	578	0.00092	182
C50ρ0.46		0.46	0.01807	534	0.00130	172
C50ρ0.38		0.38	0.01684	501	0.00154	166
C40ρ0.57	40	0.57	0.01688	447	0.00073	137
C40ρ0.46		0.46	0.01648	413	0.00091	130
C40ρ0.38		0.38	0.01589	387	0.00121	125
C30ρ0.57	30	0.57	0.01624	300	0.00051	90
C30ρ0.46		0.46	0.01582	276	0.00062	85
C30ρ0.38		0.38	0.01546	260	0.00077	82
C20ρ0.57	20	0.57	0.01218	210	0.00038	62

C20ρ0.46		0.46	0.01186	194	0.00046	59
C20ρ0.38		0.38	0.01160	182	0.00058	57

Note: P_u is the ultimate load capacity, Δ_u is the ultimate deflection, P_{cr} is the cracking load, and Δ_{cr} is the cracking deflection.

Results and Discussion

Mode of Failure and Cracking Load

Regarding the results obtained from NLFEA, the whole slab models encountered a punching shear failure; also, in-flexure cracks appeared beginning from the loading plates and stretched towards the slab models' edges. The punching shear failure was a brittle type located nearby the loading plates, and it happened when the load reached its ultimate failure level (**Figure 3**); the failure was succeeded by a punching shear cone at the lower side (tension), as illustrated in **Figure 3**. From another side, **Table 1** displays the models' summarized outcomes, regarding: at-ultimate capacity of load, at-ultimate deflections, load of cracking, and cracking deflections. **Table 1** indicated that the load of cracking became less when the reinforcement's spacing was higher; whereas, it reduced when the concrete's strength was lowered.

Figure 3. *Crack Patterns of Isometric Top View*

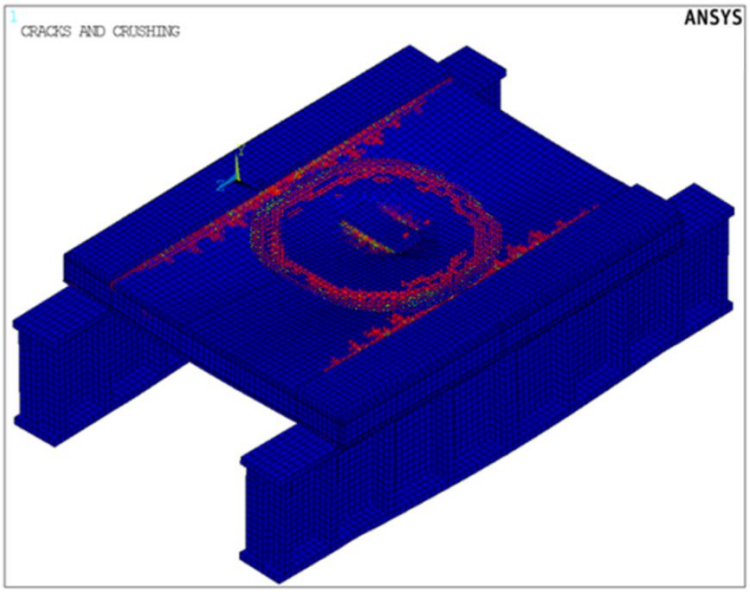

Figure 4. Typical Slabs' Diagrams of Load vs. Deflection

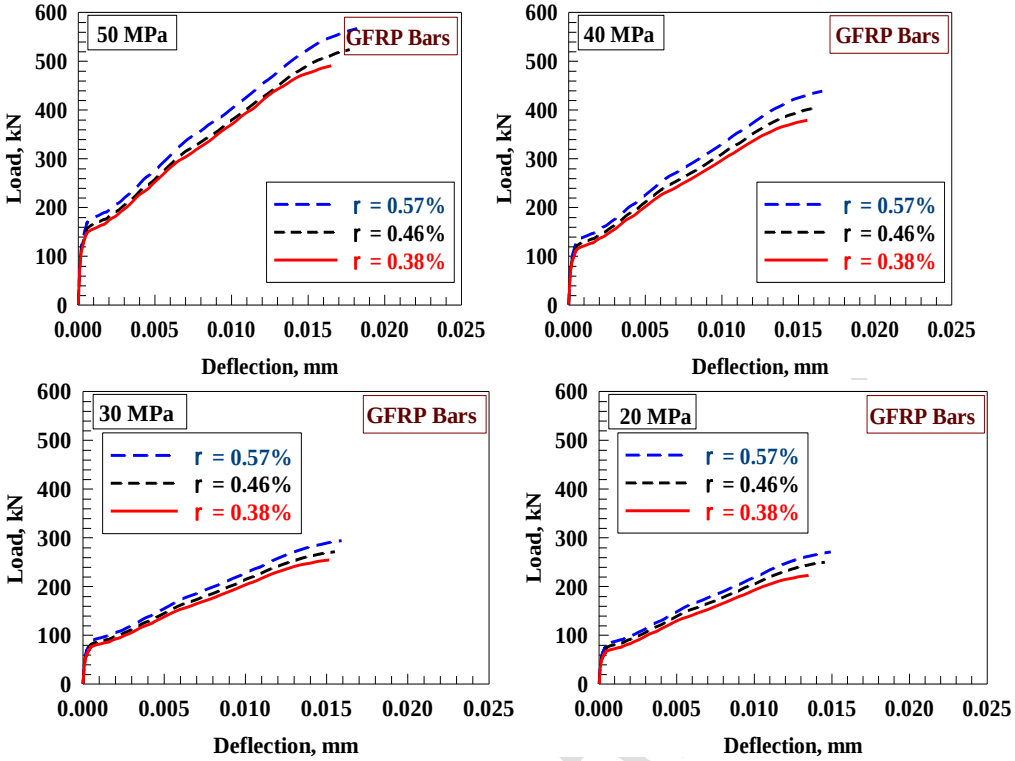

Load Deflection Behavior and Ultimate Load Capacity

The diagrams of load vs deflection (**Figure 4**) is dividend to: 1) the before-cracking part, which starts at the no load (zero) point and continues till the point at which the crack appears; and 2) the after cracking part, which begins the cracking's appearance point and continues till failure. in the latter part, the in-flexure cracks stretch in the concrete's tensile surface, along with big deflections. **Figure 4** elucidates the slab model's diagrams of load vs deflection. The diagrams indicated that the strengthened-with-GFRP-bars slab models had the least level of load and deflection. The bars of glass-FRP minimized the deflection and tolerated additional loads, where the at-ultimate capacity enhanced. This, in sequence, improved the slab models' response. Thus, strengthening bridge systems with bars of glass-FRP, at room's temperature, resulted in: (a) adding more in-compression strength per: unit of cost, unit of weight, and unit of volume; (b) enhancing the modulus of elasticity, leading to reducing deflection; and (c) increasing the in-tension strength. Further, the bars of glass-FRP improved the slabs' qualities, including: in-compression and in-tension strengths, stiffness, and modulus of the high-strength concrete. This made it possible to obtain the targeted capacity with less dimensions, which resulted in saving minimizing the level of loading to be withstood by other supports. Thus, it could be deduced that utilizing 0.38% or 0.46% of reinforcing bars of glass-FRP and concrete's strength of 39.2 MPa dissolved the issue of the ultimate load capacity; while utilizing 0.46% of glass-FRP bars and concrete's strength of 36.9 MPa solved the serviceability problem. Also, it was found that and strengthening deck slabs with glass-FRP made the slab

decks highly strong, last longer, highly anti-corrosion, and more economic with regard to construction and maintenance.

Strains in Reinforcement and Concrete

Figure 5 demonstrates the relation between the load and the maximum level of strain for the both of concrete and reinforcement. Prior to the initiation of cracking, the whole slab models exhibited nearly identical levels of strain within concrete and reinforcement. Post the emergence of cracking, the models showed various strain levels were. When the models encountered failure, the strengthened-with-steel slab models had the highest level of strains in the transversal strengthening at the bottom side; that was because the reinforcing steel yielded, as illustrated in **Figure 5**. This indicated that the strains, in concrete and reinforcment, enhanced when more reinforcing steel was used.

Figure 5. *Typical Diagrams of Load vs Strain for Slab Models reinforced with different spacing*

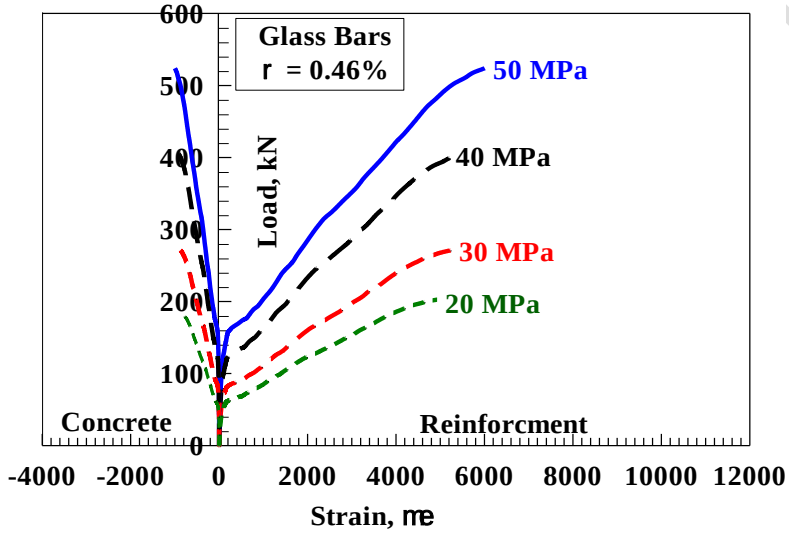

Conclusions

In light of the outcomes of this study, the following have been concluded:

1) The whole simulated-through-NLFEA slab models encountered a failure of punching shear type which resulted in decreasing the needed quantity of reinforcement, which reduced the costs incurred upon constructing strengthened-with-GFRP RC bridge's deck slabs. Also, the models showed identical patterns of cracking. The reason of this type of failure and patterns of cracking was, possibly, that the concrete was highly strong which resulted in a stronger reinforcement-concrete bonding.

2) Using bars of glass-FRP, to strengthen bridge's deck slabs, resulted in an enhancement in the models' response, compared to when using steel, and improved the levels of strength and deflection. Further, strengthening the bridge's deck slabs with bars of glass-FRP superiorly affected the slabs' at-ultimate load, elastic stiffness, stiffness after cracking, elastic energy absorption, and after-cracking energy; however, the effect was minor on the at-ultimate deflection, in comparison to models strengthened with steel.
3) In the research in hand, the simulated study models – using NLFEA – effectively and reasonably predicted the response of damaged-by-heat RC bridge's deck slab models that were strengthened with bars of glass-FRP and exposed to concentrated loads, with regard to: patterns of cracking, mode of encountered failure, and at-ultimate strength.
4) In the simulated slab models, the levels of strain, within reinforcement as well as concrete, were influenced by: high temperatures, ratio of reinforcement, and type of reinforcement. The results showed that the highest within-reinforcing-bar strain level at failure, in the strengthened-with-GFRP slab models, did not reach 50% of at-ultimate strain. It is worth noting that the highest level of strains had been taken from slabs with the least ratio of transversal reinforcement at the bottom side.

References

[1] A. Acciai, A. D'Ambrisi, M. De Stefano, L. Feo, F. Focacci, R. Nudo, Experimental response of FRP reinforced members without transverse reinforcement: failure modes and design issues, Composites Part B 89 (2016) 397–407.
[2] M. Ju, H. Oh, J. Sim, Indirect fatigue evaluation of CFRP-reinforced bridge deck slabs under variable amplitude cyclic loading, KSCE J. Civil Eng. 1–10 (2016).
[3] V.K. Kodur, L.A. Bisby, S.H. Foo, Thermal behavior of fire-exposed concrete slabs reinforced with fiber-reinforced polymer bars, ACI Struct. J. 102 (6) (2005) 799.
[4] V.K.R. Kodur, D. Baingo, Fire resistance of FRP reinforced concrete slabs: institute for research, Construction (1998).
[5] M. Robert, B. Benmokrane, Behavior of GFRP reinforcing bars subjected to extreme temperatures, J. Compos. Constr. 14 (4) (2009) 353–360.
[6] V. Kodur, L. Bisby, M. Green, Preliminary guidance for the design of FRP strengthened concrete members exposed to fire, J. Fire. Prot. Eng. 17 (1) (2007) 5–26.
[7] Hamed Ashrafi, Milad Bazli, Esmaeil Pournamazian Najafabadi, Asghar Vatani Oskouei. The effect of mechanical and thermal properties of FRP bars on their tensile performance under elevated temperatures. Construction and Building Materials 2017; 157(1): 1001-1010

[8] Sandor Solyom, Matteo Di Benedetti, Maurizio Guadagnini, György L. Balázs. Effect of temperature on the bond behaviour of GFRP bars in concrete. Composites Part B: Engineering 2020; 183(1): 107602
[9] Katz A, Berman N, Bank LC. Effect of high temperature on bond strength of FRP rebars. J Compos Constr 1999; 3(2): 73–81.
[10] Calvet V, Valcuende M, Benlloch J, Cánoves J. Influence of moderate temperatures on the bond between carbon fibre reinforced polymer bars (CFRP) and concrete. Constr Build Mater 2015; 94(1): 589–604.
[11] Yunovich, M. and Thompson, N.G. Corrosion of highway bridges: Economic impact and Control methodologies. Concrete International 2003; 25(1): 52-57.
[12] Intelligent Sensing for Innovative Structures (ISIS). Durability of fiber Reinforced polymers in civil infrastructure. Durability monograph. Canadian Network of centers of excellence on intelligent sensing for innovative Structure. MB (Canada): University of Manitoba; 2006.
[13] Kim, Yun Yong, Gregor Fischer, and Victor C. Li. Performance of bridge Deck link slabs designed with ductile engineered cementitious composite. Structural Journal 2004; 101(6): 792-801.
[14] Canadian Standard Association (CSA). Specification for fiber-reinforced Polymers. CAN/CSA S807-10. Rexdale, Ontario, Canada; 2010. 27 p.
[15] El-Gamal S. Behavior of restrained concrete bridge deck slabs reinforced with reinforcing bars under concentrated, load. Ph.D. Thesis, Sherbrooke (Quebec): Department of Civil Engineering, Université De Sherbrooke; 2005. 227 p.
[16] Canadian Standard Association (CSA). Canadian Highway Bridge design Code. CAN/CSA-S6-06. Rexdale Ontario, Canada; 2006.
[17] El-Ragaby A. Fatigue behavior of concrete bridge deck slabs reinforced with Glass FRP reinforcing bars. Ph.D. Thesis, Department of Civil Engineering, Université de Sherbrooke, Sherbrooke, Quebec; 2007. 171 p.
[18] Rajai Z. Al-Rousan, Mohammad Alhassan, Razan Al-wadi. Nonlinear finite element analysis of full-scale concrete bridge deck slabs reinforced with FRP bars. Structures 2020; 27(1): 1820-1831
[19] Tedesco, Joseph W., J. Michael Stallings, and Mahmoud El-Mihilmy. Finite Element method analysis of a concrete bridge repaired with fiber reinforced Plastic laminates. Computers & Structures 1999; 72(1-3): 379-407.
[20] Amir Gheitasi, Devin K. Harris. Performance assessment of steel–concrete composite bridges with subsurface deck deterioration. Structures 2015; 2(1): 8-20.
[21] M. Mabsout; R. Jabakhanji; Kassim Tarhini; and Gerald R. Frederick. Finite Element Analysis of Concrete Slab Bridges. Computing in Civil and Building Engineering 2000; https://doi.org/10.1061/40513(279)135.
[22] El-Ragaby, A., E. F. El-Salakawy, and B. Benmokrane. Finite Element Modeling of Concrete Bridge Deck Slabs Reinforced with FRP Bars. Special Publication 230 2005: 915-934.

[23] Bouguerra K., Ahmed E.A., El-Gamal S., Benmokrane B. Testing of full-scale concrete bridge deck slabs Reinforced with Fiber-Reinforced polymer (FRP) bars. Construction and Building materials 2011; 25(10): 3956-3965
[24] ANSYS Inc. (2015). ANSYS user's manual revision 9.0 SAS IP
[25] ASCE Task Committee on Concrete and Masonry Structure. State of the art report on finite element analysis of reinforced concrete, ASCE, 1982.
[26] Hemmaty, Y. Modeling of the shear force transferred between cracks in reinforced and fiber reinforced concrete structures. Proceedings of the ANSYS Conference 1998; 1(1): 1-13
[27] Huyse, L., Hemmaty, Y., and Vandewalle, L. Finite element modeling of fiber reinforced concrete beams, Proceedings of the ANSYS Conference 1994; 2(1), Pittsburgh, Pennsylvania.
[28] Kent, D.C., and Park, R. Flexural members with confined concrete. Journal of the Structural Division, Proc. of the American Society of Civil Engineers, 1971.
[29] ACI B. 318-Building code requirements for Reinforced Concrete and Commentary. American Concrete Institute International, 2014.
[30] Bathe, K. J. Finite Element Procedures. Prentice-Hall 1996, Inc, Upper Saddle River, New Jersey, ISBN-13: 978-0-979004902